Analyses and Applications of Nonlinear Liquid Systems on Vibration Isolation

Wenlung Li, Yu-Yen Wei
Department of Mechanical Engineering
National Taipei University of Technology
E-mail: wlli@ntut.edu.tw

Abstract

Softening nonlinear elements are usually effective for vibration reduction. However, most stress-train relations of structural systems are not exact and have limitation of materials and scale. On the other hand, one is desirable to develop nonlinear isolators to improve vibrations. Anticipating the effect of such a system is similar to a softening spring system, one can have a certain extend to design diverse kinds of softening spring terms. Especially, liquid is used to build isolation systems.

In this paper, three types of nonlinear liquid systems (NLS) are introduced, which are the exchange, buoyance and loading types. In fact, they are variable mass systems. The equations of motion of these systems are also derived to verify their nonlinearities. Numerical simulations are followed for several example shapes. The analysis results show that softening spring effects. An experimental model is displayed to verify its softening spring effects in the next steps. This paper gives guidelines and suggestions for using NLS as vibration isolators.

Keywords: Liquid Systems, Non-Linear Systems, Softening Spring, Variable Mass, Vibration Isolator

摘要

使用一些非線性軟性元件對於振動抑制是有效的。然而，大多數的應力應變經驗公式並不精確且有著材料以及尺寸上的侷限。因此值得發展他種的非線性隔振器來改善。吾人希望該系統效應類似於使用一軟彈簧之系統，而進一步在一定程度上可自由地設計各式各樣的軟彈簧項次。特別地是，流體將用於構成此隔振系統。

在本報告中介紹了三種型態的非線性流體系統（NLS），分別是浮力型、交換型以及承載型，他們可能爲變動質量系統。本研究也推導了這些系統運動方程式以驗證其非線性。本文對一些範例造型進行數值模擬，分析結果顯示其具有軟效應。本文展示了一種非線性流體系統的實驗架構以供未來驗證其軟效應。本文對使用非線性流體系統作爲隔振器提出一些指引與建議。

關鍵字：流體、非線性、軟彈簧、變動質量、隔振器

1. Introduction

Passive Isolators or absorbers are adopted to reduce vibrations. No matter the type of the reducing systems, they can be used only in a small frequency range. However, since the existence of nonlinearity in nonlinear systems, the natural frequency can be adjusted, hence it may be more flexible and useful.

In recent research of nonlinear passive vibration isolators, most of them using softening elements or the balance force curve behave softening so they are effective to reduce the transmissibility of oscillation of systems [1]. For example, Hunt and Nissen [2] show a system using a disc spring (cf. Figure 1) which is a typical softening spring, may have wider suppression band of frequency spectrum.

However, such softening springs usually cannot endure large deflection then hard or linear ones, especially during preloading to decrease the natural frequency of the systems [3-6]. On the other hand,

most of materials experience their stress-train relations formulas are not very reliable, which are always have limitation of material [3] and sensitive to scales [5].

It is desirable that one to consider other ways to develop systems such that they persevere "softening effects". Anticipating the increasing needs for such softening effect isolators from, the present research of attempts to exactly derive and simulate the effects of such nonlinear systems through with fluid ones.

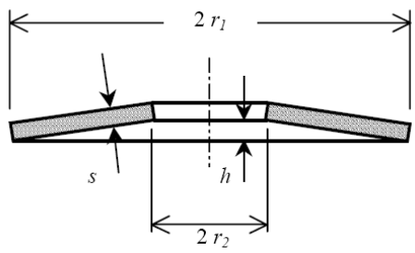

Figure 1 Geometric profile description of a disc spring.

2. Nonlinearity of vibration systems

Sources of nonlinearity can be classified into material, geometrical, or associated with nonlinear body forces or physical configuration [7]. In this paper, geometrical and configuration nonlinearities are mainly considered.

In most researches, nonlinearities more often exist in geometrical ways. Nonlinearities are brought to systems through their special profiles of elements. Generally, they are assumed to be linearly elastic when in small oscillation. However, they obey nonlinear relationships between stress and strain during large deflections. Besides, the stiffness of nonlinear elements may be softening or hardening due to the load-displacement curves.

2.1 Softening elements and their limitation

Gross [8] has shown that the load-displacement relationship of a Belleville spring (or disc spring) made by metal can be written as a function as

$$F(x) = \left(\frac{Eh^2}{1-v^2}\right)\left(\frac{sx}{nNr_1^2}\right)\left[\left(\frac{s}{h}\right)^2 + \left(1-\frac{x}{Nh}\right)\left(1-\frac{x}{2Nh}\right)\right], \quad (1)$$

where E is the Young's modulus, v the Poisson ratio, N the number of discs, n the dimensionless parameters (detail see [2, 3, 8]). Others are geometric parameters (cf. Figure 1). Chen [4] further confirmed it by using the disc spring in his frequency-adjustable absorber. However, when Tsai [3] changed the material of disc spring to plastics, the load-displacement experiment curve cannot fit the one well by substituting material parameters to equation (1). It appears even more softening. Hence equation (1) depends on the diversity of material of disc springs.

In addition, Lin [5] and Wang [6] consulted the profiles of disc and springs as well as many other softening elements, and constructed their own softening elements in their isolators. In their results, the stiffness is sensitive to the thickness of the components, and hard to give a mathematical model. They all checked the elements by CAD/CAE and confirmed by tensile tests. However, it is costly and sometimes leads to curves with a quite large spectrum, unfortunately.

Virgin et al. [9] used a highly deformed polycarbonate strip clamped together at the end and attached to a vertically oscillating base for an isolation element to reduce the motion of a supported mass. They derived the governing equations using an elastica analysis [10]. And they solved numerically the equations using a shooting method to satisfy the boundary conditions. The numerical results almost fit the experimental ones about force-deflection relationship. Numerical method may be more reliable, but it's too complex to get the right answer.

The present research attempts to find out simpler and exact rules for producing softening spring effects of vibration isolation systems.

2.2 The softening spring effects

Some configuration nonlinear systems give ideas to get the softening effects. Carrella et al. [11] used two oblique springs into their system (Figure 2). The force-displacement relation about oblique springs can be written as

$$f(x) = 2k_0(h_0 - x)\left(\frac{\sqrt{h_0^{\,2} + a^2}}{\sqrt{(h_0 - x)^2 + a^2}} - 1\right), \qquad (3)$$

which refers to a hardening curve. While they set the combined point with an offset or an initial angle of the oblique spring, it can behave softeningly. Specially, it is quasi-zero stiffness when moving near horizontal line *MN*. It has no argument about the results since the formula can be readily derived by statics. One can have the exact equation of motion of the system by equation (3) and the constant stiffness of the linear spring. One can also tune the natural frequency of the system like preloading softening elements by set different initial angle or changing different springs of different stiffnesses to get a new force-displacement curve. Chen [12] shows another case. A linear spring passing horizontally through a non-constant cross-section channel (cf. Figure 3) [12]. The force-displacement relation can be written as

$$F(x) = 4k\int_0^x f'(x)^2 dx\,, \qquad (4)$$

where $f(x)$ is the channel's profile function.

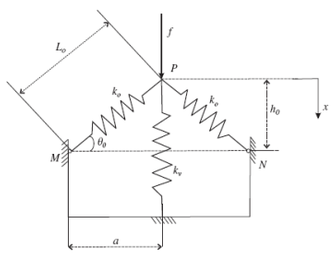

Figure 2 Schema of the oblique spring system [11].

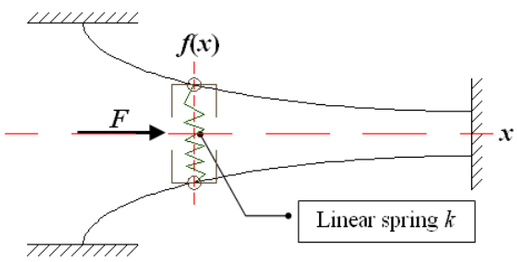

Figure 3 Linear spring moves in a variation channel.

Theoretically, one can substitute any satisfactory function into equation (4) and then get the effect of the softening spring term. Therefore, the complete behaviors can be obtained. These two examples show that one can design the spring term in certain range freely by using configuration nonlinearity. The present research even suggests one to extend the results to higher degree of freedom systems.

3. Systems using liquid

Relatively few researches consider using liquid to build isolation systems than using structural ones. The main reason may stem in hard to exactly describe the motion of liquid. However, one still can have an approximate solution under some assumptions.

Liquid preserves mass, damping and probably nonlinearity as well, due to the frame of the system. It's interesting to find out how it leads to softening effects. Since some liquid systems using Turned liquid column damper (TLCD) [13-18] have discussed about reducing horizontal vibration or rolling motion, the present research will focus mainly on vertical vibration isolation. Three types of NLS that producing softening spring effects by its configuration are discussed. Besides, they have the similar idea -- liquid flow through variation frames.

3.1 The buoyance type

According to Archimedes' principle, any object, wholly or partially immersed in a fluid, buoys up by a buoyant force equals to the weight of the fluid that displaced by the object [19]. Besides, the present research neglects surface tension (capillarity) acting on the body as the principle does in this type. One also neglects the influence of sloshing [20-22], thus assumes the steady flow and the cover of liquid to be a horizontal plane which balance instantly.

A buoyancy system (NLS-B) using a diverse dobber attached to a support system is shown in Figure 4. The relationship between the displacement x and the volume

of the fluid displaced by the dobber can be nonlinear due to the non-constant cross-sectional area of the dobber.

By the conservation of mass, cf. Figure 4, the equation of motion for undamped free vibration is

$$m\ddot{x} + kx + \rho g B(x) = m\ddot{x} + f(x) = 0\,, \tag{6}$$

where m is the total mass of dobber and support plate, k the stiffness of the linear spring, g the acceleration of gravity (adopt 9.81 m/s^2) and ρ the density of liquid. The buoyancy function can be expressed as

$$B(x) = -\int_{L_0}^{L_0-(x+\eta)} A(\xi)d\xi = A_0\eta\,, \tag{7}$$

where L_0 is the height of the dobber sink into the liquid initially, $A(\xi)$ the section profile function (cf. Figure 5) of the dobber, A_0 the constant section area of the tank and η the displacement variable of liquid cover. This paper analysis an example with a symbolic section profile as

$$A(\xi) = A_1 + s(\xi - L_0)^2\,, \tag{8}$$

which is a symmetric shape. A_1 is the section area of dobber at static surface. A sample plot of $A(\xi)$ with different coefficient s is shown in Figure 6 (S.I. unit).

If A_0 is much greater than the maximum of $A(\xi)$, which means the tank is extreme large, one can easily integrates equation (8) by letting η = 0. However, this paper considers the existence of η.

Refer to Figure 6, if s is positive, the cross-section of the dobber gets wider from $\xi = L_0$ to both sides and for negative s it gets narrower. The present research believes the softening spring effects will occur for either wider or narrower case.

In order to get a desired nonlinear element, the present research suggests that the two steps: (1) To determine the profile function of the cross sectional area; and (2) To derive a one-to-one function of x by using equation (7) to obtain parameter η. By substituting equation (8) to equation (7), one yields

$$(x+\eta)[A_1 + \frac{s}{3}(x+\eta)^2] - A_0\eta = 0\,, \tag{9}$$

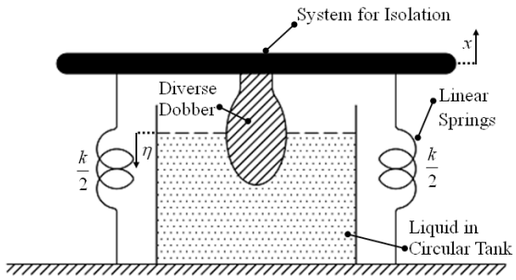

Figure 4 The forces at work in buoyancy.

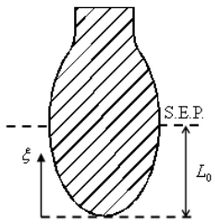

Figure 5 Diverse dobber of the system in Figure 4.

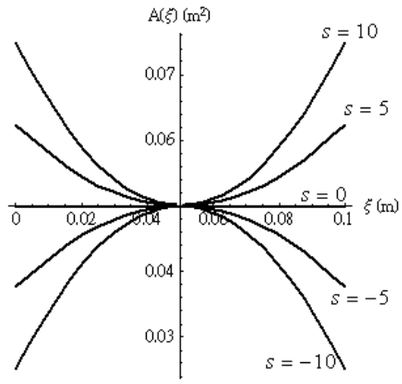

Figure 6 Plot of equation (8) for A_1 = 0.05 m^2 and L_0 = 0.05 m with different coefficient s.

which is obvious an implicit function of x. The plot that using the same parameters as in Figure 6 is shown in Figure 7. Notice that since the direction of x and η, they must be the same sign. One can only consider the curve in the first and third quadrant. Besides, the dobber is limited not to leave the liquid. In other words, it leads the limitation function to $\eta + x = L_0$. In addition, one considers the dobber always touches the liquid, it thus leads to another limitation function: $\eta + x = -L_0$. As a

consequence, the available moving range locates in the triangle regions in the first and the third quadrant, shown in Figure 7.

For an approximate solution of the curve, one is to consider small oscillations of the plate. In the mean time, the cubic terms of x and η in equation (9) are neglected. For a simple comparison, one considers the case $s = \pm 10$, shown in Figure 8. As $s = -10$, $A_0 = 0.1\text{m}^2$, $A_1 = 0.05\text{m}^2$ and $L_0 = 0.05$ m, one solves equation (9) and yields

$$\eta^*(x) = \frac{(-0.05^2 - 0.5x^2 + 0.5\sqrt{x^4 + 0.03x^2 + 0.005^2})}{x}. \quad (10)$$

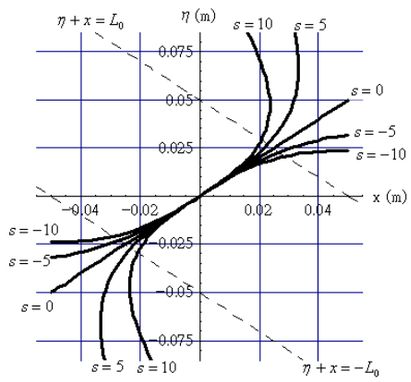

Figure 7 Plot of equation (9)

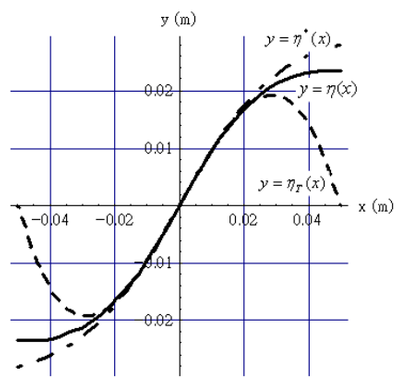

Figure 8 Comparison plot of case $s = -10$.

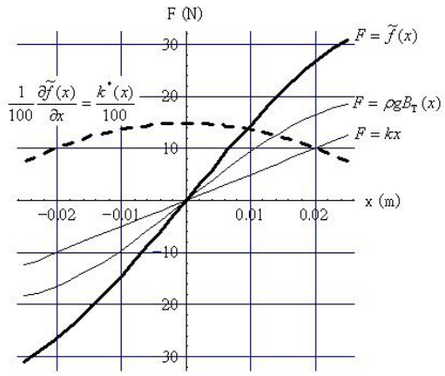

Figure 9 Force combination curve of case $s = -10$ for $k = 500$ (N/m), $\rho = 1000$ (kg/m^3).

It's convenient to use the Taylor expansion of equation (10) to have a polynomial function. Keeping up to the cubic terms, one yields

$$\eta_T(x) = x - 400x^3. \quad (11)$$

The comparison plot is shown in Figure 10. Equation (11) shows well approximation for $|x|$ less than about 0.02. One can just substitute equation (11) to equation (7) and get the approximate buoyancy variation function, which is

$$B_T(x) = A_0\eta_T(x) = 0.1x - 40x^3. \quad (12)$$

Figure 9 shows the force combination curve for the specified values, where the approximate spring term of equation (6) is determined as

$$f(x) \cong \tilde{f}(x) = kx + \rho g B_T(x) = 1481x - 392400x^3, \quad (13)$$

in which the stiffness function is

$$k^*(x) = \frac{\partial f(x)}{\partial x} = 1481(1 - 795x^2), \quad (14)$$

In this case, equation (14) is valid for $|x|$ less than ca. 0.02. Notice also that the negative stiffness function s shows a softening result which is what one is looking for.

For another case $s = 10$, using the same parameters as those in Figure 8 and deriving the relative functions, one obtains the followings:

$$\eta^*(x) = \frac{(-0.05^2 - 0.5x^2 + 0.5\sqrt{x^4 - 0.03x^2 + 0.005^2})}{x}, \quad (15)$$

$$\eta_T(x) = x + 400x^3, \quad (16)$$

$$B_T(x) = A_1\eta_T(x) = 0.1x + 40x^3, \quad (17)$$

$$f(x) \cong \tilde{f}(x) = kx + \rho g B_T(x) = 1481x + 392400x^3, \quad (18)$$

$$k^*(x) = \frac{\partial f(x)}{\partial x} = 1481(1 - 795x^2). \quad (19)$$

Plots are shown in Figures 10 and 11. Notice that the stiffness function shows a hardening result. Thus, the softening effect of NLS of the buoyance type (NLS-B) occurs only as s is negative. The works above are done with the help of the math software MATHEMETICA.

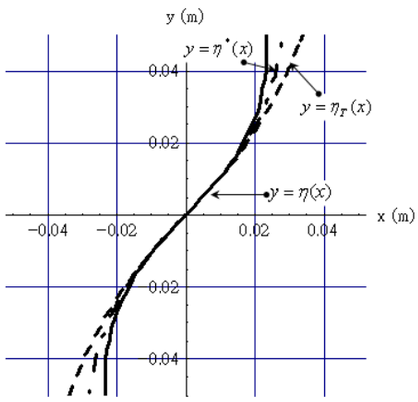

Figure 10 Comparison plot of case s = 10.

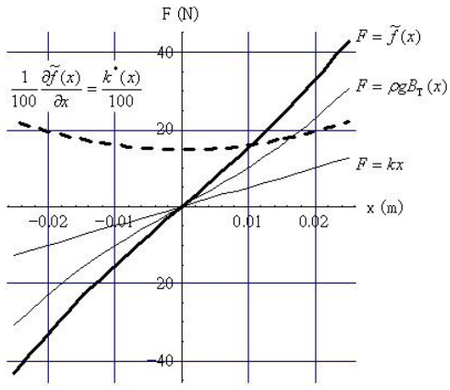

Figure 11 Force combination curve of case s = 10 for k = 500 (N/m), ρ = 1000 (kg/m^3).

Specially, one further considers the case s = 0, with the diameter of the dobber d_0 and the diameter of the tank D_0. Solving equation (8) and substituting into equation (7), one has

$$m\ddot{x} + [k + \rho g \frac{\pi D_0^{\,2} d_0^{\,2}}{4(D_0^{\,2} - d_0^{\,2})}]x = 0, \quad (20)$$

which shows a linear equation as one expect.

It's rational to guess that if this NLS-B perseveres softening spring effects, the cross-section area of the dobber should get narrower from the static surface. Theoretically, one can design a softening spring term whatever one wants by using equation (7). If one neglects the spring (i.e. k = 0), the rule of the dobber shape still keeps the same. However, one may need to take the limit of the maximum loading into account. One can use more dobbers in parallel or a bigger one in this type to enhance the softening effect.

3.2 The exchange type

The word "exchange" here means the liquid can flow between a few manifolds or chambers in the system. System using TLCDs has been studied. They discussed the optimal factors of TLCD to reduce the horizontal vibration [13-16], rotational motion [17] or even both [18] of a system which has usually been linearized.

A U-type TLCD system is shown in Figure 12 [14], which furthermore adds pressure element. If one ignores the gas pressure in the uniform U-tube, it's a linear system and the natural frequency [15] of U-tube is derived as

$$\omega_n = \left(\frac{2g}{l}\right)^{1/2}, \quad (21)$$

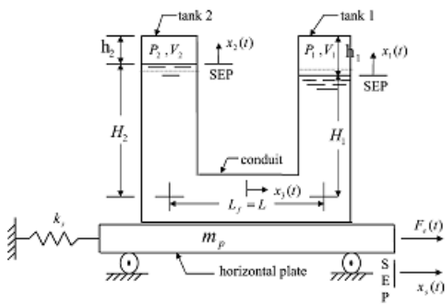

Figure 12 A horizontal plate carrying a U-type TLCD [14]

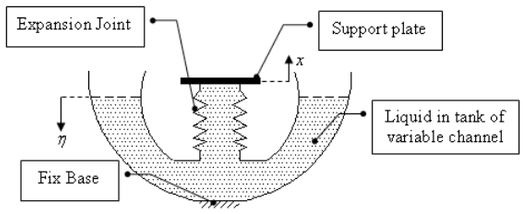

Figure 13 Variation channel with expansion joint.

where l is the total length of the liquid and g the acceleration of gravity. Even one considers the gas pressure or for non-uniform sections of vertical and horizontal region of the tube, the restoring force of TLCD system is still linear. Deng [23] showed that by non-uniform sections of input and output side like jacks using oil pressure, the vertical vibration may be reduced well for the specific ratio of area in certain conditions, but the restoring force of the system is linear as well.

The present research then guesses if the exchange type brings up nonlinearity, it does not depend on the different sections of chambers, but at least one side has diverse section through the channel.

A Single D.O.F. NLS of exchange type (NLS-E) with variation channel is revealed by improving the model Santillan et al. [10] revealed. The sketch is shown in Figure 13. The assumptions of liquid are the same as in section 3.1. The cover of liquid will flow following the diverse channel with η witch can be derived to a one-to-one function of x, which is the displacement of the plate. Since the height of liquid may vary nonlinearly, it will lead to various nonlinear terms that corresponding to the profiles.

3.3 Loading type

Considering a similar idea, the loading type (NLS-L) further uses the mass of liquid, and the system can behave a variable mass term. In fact, a typical system was introduced by Rao [24] and Den Hartog [25] shown in Figure 14. The system contains two circular tanks, a plate slides in one of the tanks, a linear spring for supporting the plate, and some kind of liquid storage in the tank. The instant loading of the system (dashed rectangle) depends on the displacement x, and so nonlinearity may appear in the mass term. The present research generalizes the system to a variation profile. But the first important work is to discuss whether the specific diameter ratio of the original system may lead to softening effect or not.

The demonstration structure is shown in Figure 15. A transfer region is added into the original system for flowing smoothly of the liquid. The assumption is the same as the case of NLS-B and NLS-E. To derive the equation of motion, one uses the Lagrange Equation. Or, the kinetic energy can be written as

$$T = \frac{1}{2}[m_0 + \rho A_0(L_0 - x) + \rho A_0\alpha^2(L_1 + \alpha^2 x) + \rho A_0{}^2 \int_0^L \frac{d\xi}{A(\xi)}]\dot{x}^2 \quad , \qquad (22)$$

where ρ is the density of liquid, α the diameter ratio. And α satisfies $\alpha^2 = A_0/A_1$, which is area ratio.

Assume the bases are all fixed (i.e. $u(t) = 0$), the potential energy can be written as

$$V = \frac{1}{2}[k + \rho A_0 g(1-\alpha^2)]x^2 , \qquad (23)$$

where g is acceleration of gravity. By the principle of conservation of mass, one can easily derive the variable $\eta(x) = \alpha x^2$. By substituting it into the process for deriving kinetic and potential energy, the variable is vanished and the system becomes single D.O.F. system.

Consider the transfer region of the system with the function $A(\xi) = A_0 + (A_1 - A_0)(\xi/L)^2$, by substituting it and equation (22), equation (23) into Lagrange equation, yields

$$[m_0 + \rho A_0 (L_0 + \alpha^2 L_1 + \alpha L)]\ddot{x} + [k - (1-\alpha^2)\rho A_0 g]x + \rho A_0 (\alpha^4 - 1)[0.5\dot{x}^2 + x\ddot{x}] = F(t) \quad (24)$$

which is the equation of motion.

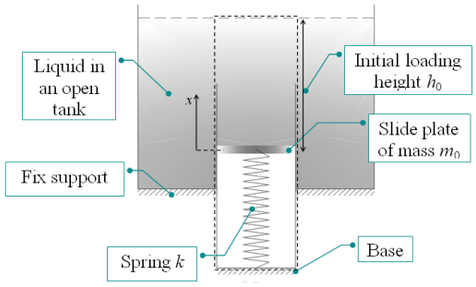

Figure 14 Variable mass system [13].

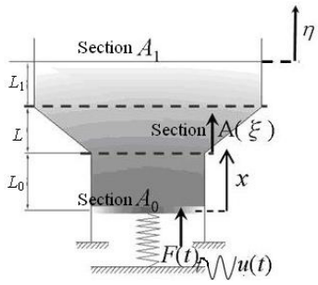

Figure 15 Different diameter tanks with transfer region.

The nonlinear term appears at the LHS is from the nonlinear momentum. The straight velocity profiles are different for the two section areas. And, the mass variable and the loading vary with the variable x.

A standard form with viscous damping is then

$$\ddot{x} + 2\zeta\omega_0\dot{x} + \omega_0^2 x + \gamma\omega_0^2(0.5\dot{x}^2 + x\ddot{x}) = f(t), \quad (25)$$

where the natural frequency is

$$\omega_0 = \sqrt{g(P_k + \alpha^2 - 1)/[L^*(P_m + 1)]}, \quad (26)$$

with the nondimensional parameters

$$P_k = \frac{k}{\rho A_0 g}, P_m = \frac{m0}{\rho A_0 L^*}. \quad (27)$$

The equivalent length in equation (28) is defined as

$$L^* = L_0 + \alpha^2 L_1 + \alpha L, \quad (28)$$

and the nonlinear factor is

$$\gamma = g^{-1}\frac{\alpha^4 - 1}{P_k + \alpha^2 - 1}. \quad (29)$$

Though the numerator of equation (26) may be negative or positive, for stability of the system requires the natural frequency to be a positive real number, hence $P_k + \alpha^2 > 1$ and the sign of γ is due the diameter ratio α (or area ratio α^2). A contour plot is shown in Figure 16 for an example. Notice that the region is only valid in $P_k + \alpha^2 > 1$ (i.e. the right upper side above the oblique line $P_k + \alpha^2 = 1$). Besides, γ is negative over the left side ($\alpha < 1$) of the straight line $\alpha = 1$ and positive over the right side $\alpha > 1$.

The system of equtaion (25) is applied by a swept-sine analysis to verify whether the natural frequency will shift with the nonlinear factor or not. The SIMULINK model is shown in Figure 17.

For reason of demonstration, one sets the frequency range of a chirp signal from 0 to $4\omega_0$ in 20 sec as same as sampling time (i.e. the precision of response spectrum is 0.05 Hz) and the sampling frequency to $10\omega_0$ since it's enough. Fix-step solver is ode3 (Bogacki-Shampine method).

The spectrum of the Chirp signal is shown in Figure 18, and a typical output spectrum with nonlinear factor is shown in Figure 19. The Plot of the magnification factor to the nonlinear factor is shown in Figure 20 and Table 2.

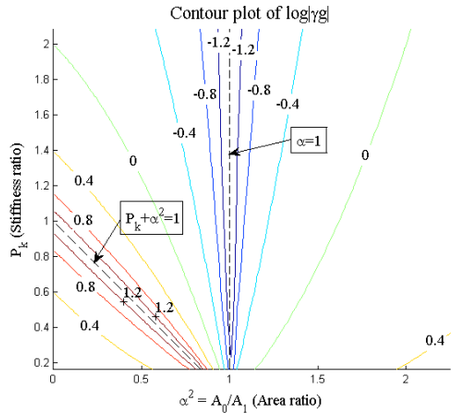

Figure 16 Contour Plot about equation (29).

Analysis results show that for the larger magnitude of nonlinear factor, the less magnification factor. It may due to the last nonlinear term in equation (25).

However, for a damped system it shows no different. On the other hand, the max response frequency is still kept the same, and this phenomenon holds for other original natural frequencies or magnitudes when applying chirp signals A_{m}. The reason can be refer to the static status, i.e. $\dot{x} = \ddot{x} = 0$, since the linear relationship between the balance force and the displacement x.

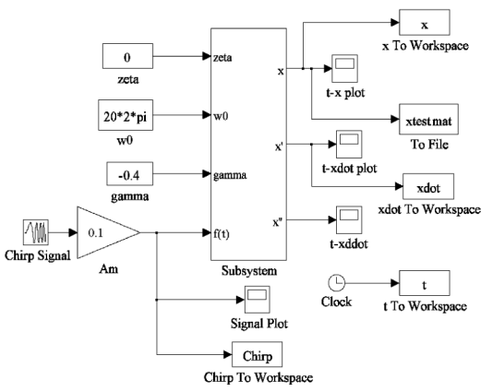

Figure 17 SIMULINK model of equation (25).

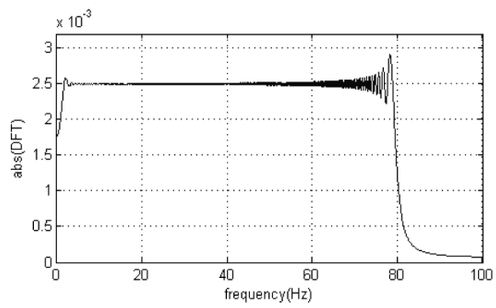

Figure 18 Frequency spectrum of chirp signal.

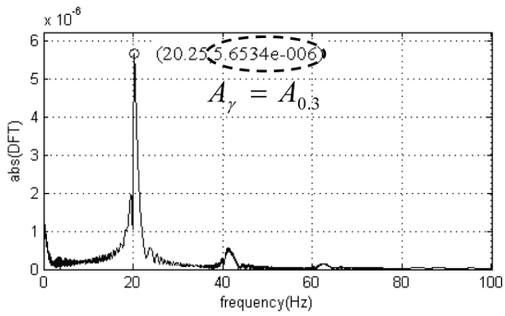

Figure 19 Outputs spectrum for parameters $\omega_0 = 40\,\pi$, $\zeta = 0$, $\gamma = 0.3(\alpha > 1)$, $A_{\mathrm{m}} = 0.1$.

Table 2 Magnification factor $M_\gamma = A_\gamma \omega_0^2 / A_{\mathrm{m}}$

γ	-0.3	-0.2	-0.1	0	0.1	0.2	0.3
M_γ	0.860	1.255	1.369	1.401	1.376	1.269	0.893
$\frac{M_\gamma}{M_0}$	61.36 %	89.58 %	97.71 %	100%	98.2 %	90.55 %	63.71 %

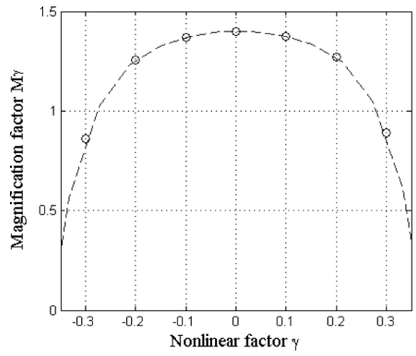

Figure 20 Plot of magnification to nonlinear factor.

Although the amplitudes of the vibration do not reduce obviously as the nonlinear factor varies, the non-constant section profiles do keep the characteristics of softening springs. Figure 21 shows a general structure. It's unnecessary to make a variation section container, but use a cylinder tank with a variation section core to achieve the variation section frame. The kinetic energy of such a system can be written as

$$T = \frac{1}{2}[m_0\dot{x}^2 + \rho A_0(L_0 - x)\dot{x}^2 + \rho A_0^2\dot{x}^2 \int_0^{L_1+\eta} \frac{d\xi}{A(\xi)}]. \quad (30)$$

Notice that the upper limitation of integration is a constant in equation (22) while a function of x in equation (30). Assume the base is fixed (i.e. $u(t) = 0$), the potential energy can be written as

$$V = \frac{1}{2}[k - A_0\rho g]x^2 + \rho g \int_{L_1}^{L_1+\eta} A(\xi)(\xi - L_1)d\xi\,, \quad (31)$$

which is more complex than equation (23), and may lead to a nonlinear spring term since the last term of it.

Equation (30) and equation (31) shows the general form of energy for the general NLS-L. The first work is also to derive the displacement of liquid cover $\eta(x)$. According to the principle of conservation of mass yields

$$\int_{L_1}^{L_1+\eta} A(\xi)d\xi = A_0 x\,. \tag{32}$$

For any section profile function $A(\xi)$, the equation of motion can be determined by Lagrange Equation. The equation of motion with damping force can be written in a general form as

$$\ddot{x} + 2\zeta\omega_0\dot{x} + \omega_0^{\,2}[f(x) + g(x)\dot{x}^2 + h(x)\ddot{x}] = f(t)\,. \tag{33}$$

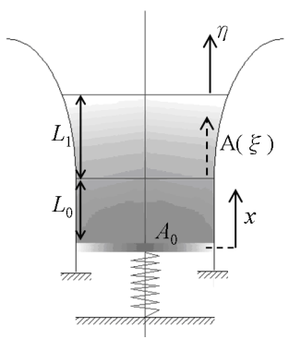

Figure 21 Demonstration of a general structure.

To solve whole term of equation (33) is not necessary for confirming the softening spring effects. Consider the system is in static status (i.e. $\dot{x} = \ddot{x} = 0$), the relationship between balance force and displacement x is only due to the third term of equation (31). For example, one can imagine that for a wider section tank from static position, the height of the liquid gets shorter hence the restoring force will be softening.

An experimental structure in introduced in Figure 22, which is used to verify the NLS-L in the future. A non-constant cross-section core is put inside the tube instead of making a variation profile tank. External force from a shaker acts through a load cell to the rods and then to slide plate. One can consider a machine attaches to the slide plate, and the oscillation of it can be seen as the energy from the shaker.

By the reference of NLS-B, the cores as modules are considered to make the section area vary from narrow to wide for softening spring effects. Some examples of core are shown in Figure 23. Specially, type (a) will be used to verify the area ratio effect this paper discussed.

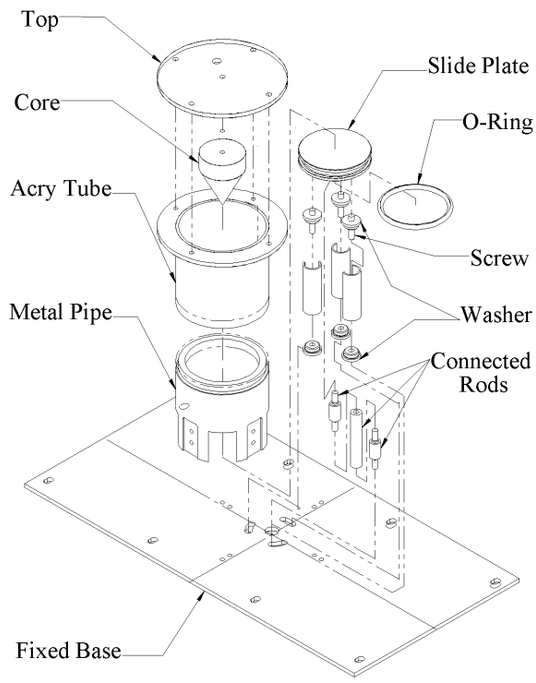

Figure 22 Demonstration of the NLS-L.

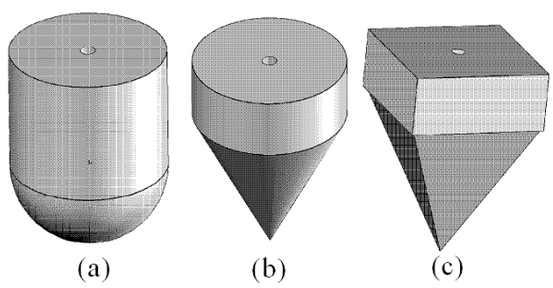

Figure 23 Cores of NLS-L. (a) Cylinder with diversion head, (b) Cone, (c) Square based pyramid.

4. Conclusion

Three types of NLS, which consider using liquid in the system for vibration isolation, were discussed in this paper. Anticipating improving the disadvantages of geometric softening elements, the present research presumed idea non-viscid liquid. NLS-B perseveres softening spring effects due to the variation of buoyancy, and can be used as base isolation. On the other hand, NLS-E reveals that liquid flow through a diverse frame or between different size regions may lead to nonlinearity. Furthermore, NLS-L shows that non-uniform tanks of input and output is a linear system, and further suggests a diverse tank as the same idea as NLS-E.

Once the profiles (e.g. dobbers of NLS-B, tanks of NLS-E, cores of NLS-L) of the elements are decided, the equation of motion as well as the nonlinear effects (usually designs to softening) are determined. NLS-B may be the easiest one to derive and the form is similar to a softening structure system. However, once the energy of liquid is considered in NLS-E and NLS-L, they lead to more complicated terms in the system equations. The terms mainly stem from the variable of mass or loading, and may have better performance for isolation.

5. References

[1] Ibrahim R A. Recent advances in nonlinear passive vibration isolators. Journal of Sound and Vibration, 2008; 314: 371-452.

[2] Hunt J B, Nissen J C. The broadband dynamic vibration absorber. Journal of Sound and Vibration, 1982; 83: 573-578.

[3] 蔡忠瑾。應用非線性元件模組之創新微振避振平台研發。碩士論文，國立臺北科技大學機電整合研究所，2006。

[4] 陳信宏。頻率可調式非線性微吸振器之研究。碩士論文，國立臺北科技大學製造科技研究所，2003。

[5] 林逸倫。非線性元件於隔振之效應分析及驗證研究。碩士論文，國立臺北科技大學製造科技研究所，2008。

[6] 王信富。應用非線性元件於高架地板之創新設計隔振器研究。碩士論文，國立臺北科技大學機電整合研究所，2008。

[7] Thomsen J J. Vibrations and stability, 2nd edition. New York: Springer. 2003.

[8] Gross S. Calculation and design of metal springs. London: Chapman & Hall. 1966.

[9] Virgin L N, Santillan S T, Plaut R H. Vibration isolation using extreme geometric nonlinearity. Journal of Sound and Vibration, 2008; 315: 721-731.

[10] Santillan S, Virgin L N, Plaut R H. Equilibria and vibration of a heavy pinched loop. Journal of Sound and Vibration, 2005; 288: 81-90.

[11] Carrella A, Brennan M J, Waters T P. Static analysis of a passive vibration isolator with quasi-zero-stiffness characteristic. Journal of Sound and Vibration, 2007; 301: 678-689.

[12] 陳予恕。非線性振動。北京：高等教育，2002。

[13] Balendra T, Wang C M, Cheong H F. Effectiveness of tuned liquid column dampers for vibration control of towers. Engineering Structures, 1995; 17: 668-675.

[14] Wu J S, Hsieh M. Study on the dynamic characteristic of a U-type tuned liquid damper. Ocean Engineering, 2002; 29: 689-709.

[15] Chaiviriyawong P, Webster W C, Pinkaew T, Lukkunaprasit P. Simulation of characteristics of tuned liquid column damper using a potential-flow method. Engineering Structures, 2007; 29: 132-144.

[16] 吳佳璋、梁育誠。承受多個外力之阻尼結構系統的減振研究。應用聲學與振動學刊，2009，1卷 1 期，39-49 頁。

[17] Wu J C, Wang Y P, Lee C L, Liao P H, Chen Y H. Wind-induced interaction of a non-uniform tuned liquid column damper and a structure in pitching motion. Engineering Structures, 2008; 30: 3555-3565.

[18] Shum K M, Xu Y L. Multiple tuned liquid column dampers for reducing coupled lateral and torsional vibration of structures. Engineering Structures, 2004; 26: 745-758.

[19] Wikipedia. Buoyancy. 2010. From http://en.wikipedia.org/wiki/Buoyancy

[20] 李台綾。圓柱形儲槽之非真圓公差對動態特性之影響研究。碩士論文，國立臺北科技大學自動化科技研究所，2004。

[21] Jin Q, Li X, Sun N, Zhou J, Guan J. Experimental and numerical study on tuned liquid dampers for controlling earthquake response of jacket offshore platform. Marine Structures, 2007; 20: 238-254.

[22] Ikeda T, Murakami S. Autoparametric resonances in a structure/fluid interaction system carrying a cylindrical liquid tank. Journal of Sound and Vibration, 2005; 285: 517-546.

[23] 鄧錦坤。應用液體體積轉換於導引懸吊系統的結構設計與性能分析。博士論文，逢甲大學機械與航空工程研究所，2008。

[24] Rao S S. Mechanical vibrations, 4th edition. New Jersey: Prentice Hall. 2004.

[25] Den Hartog J P. Mechanical vibrations, 4th edition. New York: Courier Dover. 1985.